Hindawi
International Journal of Aerospace Engineering
Volume 2022, Article ID 8063786, 8 pages
https://doi.org/10.1155/2022/8063786

Research Article

Application of Stewart Platform in the Low-Frequency Vibration Characteristic Test of Space Truss Deployable Antenna on Satellite

Hui Wang, Jiang Zhao, Yonggang Xue, Zhirong Huang, Shikun Zheng, and Xiaofei Ma

China Academy of Space Technology (Xi'an), Xi'an, China

Correspondence should be addressed to Hui Wang; wangh23@cast504.com

Received 13 April 2022; Revised 20 May 2022; Accepted 17 June 2022; Published 4 July 2022

Academic Editor: Adel Ghenaiet

The space truss deployable antenna has low natural frequency, multi-closed-loop, and multiredundant structure characteristics, which is a kind of flexible antenna. It is hard to obtain the vibration characteristics under low frequency by finite element analysis or conventional shaking table test. To verify the structure characteristics of the antenna in the folded state below 2 Hz, a low-frequency vibration system is established based on the 6-DOF Stewart platform. Rotation matrix analysis method was adopted to obtain the platform's velocity and acceleration characteristics. Then, a low-frequency vibration test was carried out on the platform. The results show that the natural frequency of the antenna is 1.51 Hz and the maximum dynamic displacement is 140.6 mm, which provides a certain foundation for the further development of the space truss antenna.

1. Introduction

The space truss deployable antenna is a large-scale mesh deployable truss structure with high storage ratio and large deployment stiffness. The main structure is composed of multiple tetrahedral frame elements with energy storage springs. These basic tetrahedral retraction and deployment elements share nodes, and the retraction movement is associated to form a multi-closed-loop and multiredundant space structure [1–3]. The antenna is folded and fixed before launch, and the expansion is realized by a spring driving on the orbit to form a paraboloid. The antenna has good strength, stiffness, and high deployment reliability [4, 5]. It can flexibly construct the truss system by changing the number of basic truss elements or adopting different connection methods. Due to the stiffness characteristics of the structure and the freedom of the configurable truss structure, many research institutions have carried out relevant technical research at present [6–9].

Due to the limitation of rocket payload space, the large aperture antenna needs to be folded. The antenna must be able to withstand the vibration from the rocket or itself without damage during launch. The general method is to use the finite element analysis method or shaking table test to simulate the real vibration environment during transportation [10].

The truss antenna contains a large number of rods, ropes, and hinges, and its dynamic model is complex, which brings great challenges to the finite element solution [11]. At the same time, to reduce the weight of the antenna, the lightweight carbon fiber composite is usually used as the rod material, which will inevitably reduce the strength of the rod and make the flexibility of the antenna more obvious. The fundamental frequency of the antenna in the folded state is usually below 2 Hz. Therefore, the vibration test of the truss antenna puts forward higher requirements for the working frequency and output load of the shaking table.

Limited by the current low-frequency shaking table technology, the frequency range of the small shaking table is $2 \sim 10$ kHz and that of the large shaking table is $5 \sim 2$ kHz. Therefore, it is difficult to realize the low-frequency vibration assessment [12]. The Stewart platform is a spatial 6-

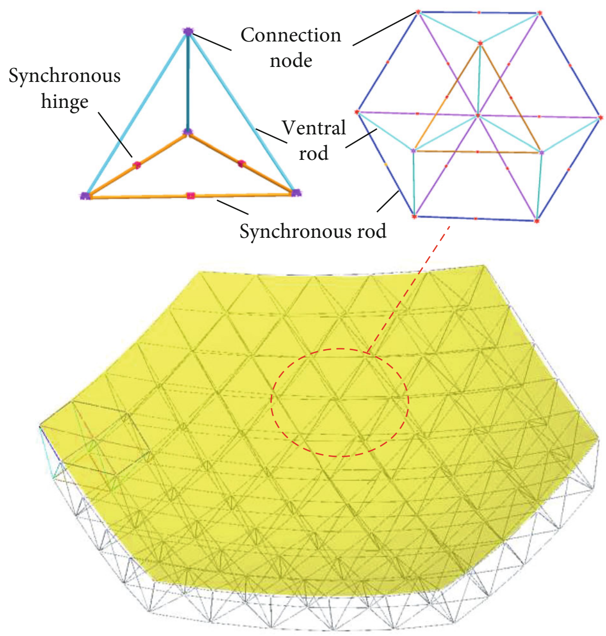

Figure 1: Frame units with tetrahedral element.

DOF parallel mechanism. By controlling the independent movement of six telescopic cylinders, it can simulate various attitude responses of the spacecraft during space flight, especially the low-frequency vibration during launch. It has become an important simulation test device for dynamic reliability research of aerospace equipment [13, 14].

In this paper, a low-frequency vibration characteristic test platform suitable for the space truss antenna is built based on Stewart platform, and relevant low-frequency tests are carried out to obtain the fundamental frequency and dynamic displacement in the stowed state, which provide a certain foundation for the further development of the space truss antenna.

2. Antenna's Structure Characteristics

The antenna is composed of reflector, truss, and a metal mesh. The reflector truss is composed of several frame units. Each unit adopts a tetrahedral element, which is composed of web members, folding rods, connection nodes, and torsion springs, as shown in Figure 1.

The three folding rods can be folded symmetrically around the middle, and the middle of each folding rod is provided with a hinge, which contains a spring. When the tetrahedron is folded, the spring element of the folding rod stores energy and acts as the driving force of the tetrahedron unit when it is deployed. The deployable state and fold state of the antenna are illustrated in Figure 2.

3. Kinematics Analysis of Stewart Platform

3.1. 6-DOF Stewart Platform. The 6-DOF Stewart parallel platform is mainly composed of the load platform, base platform, and six driving cylinders. Each driving cylinder is connected to the load platform and base platform, respectively, by a hinge. According to different hinge modes, it can be divided into ball joint S-P-S (sphere joint-prismatic joint-sphere joint) type and universal joint U-P-S (universal joint-prismatic joint-sphere joint) type.

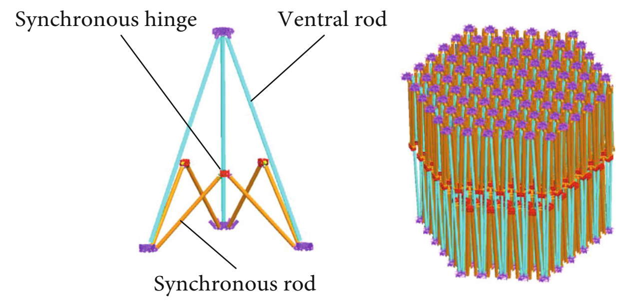

Figure 2: Fold state of the antenna.

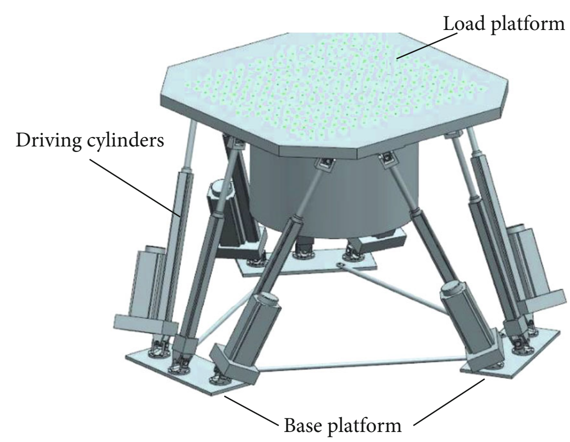

Figure 3: 6-DOF Stewart parallel platform.

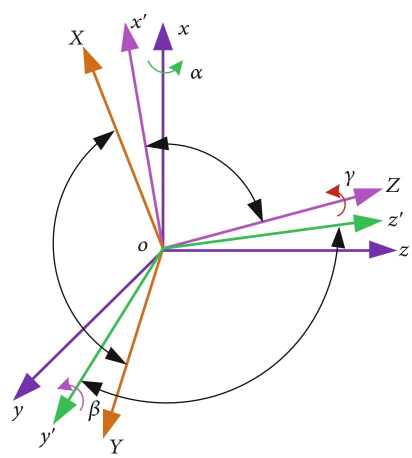

Figure 4: Cardan angle coordinate system schematic diagram.

The working platform includes an upper platform, lower platform, load mounting plate, upper and lower connecting hinges, servo actuator, auxiliary cylinder, and base, as shown in Figure 3. The servo actuator is composed of an electric cylinder and motor. The servo actuator receives the control signal and works on the platform to make the upper platform realize longitudinal, heel, yaw, lifting, transverse, and

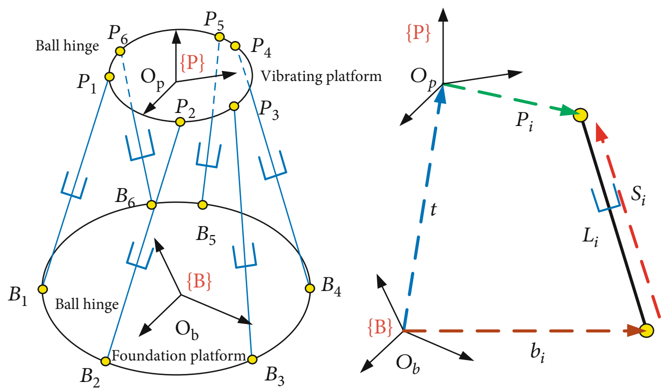

FIGURE 5: Coordinate system of Stewart platform.

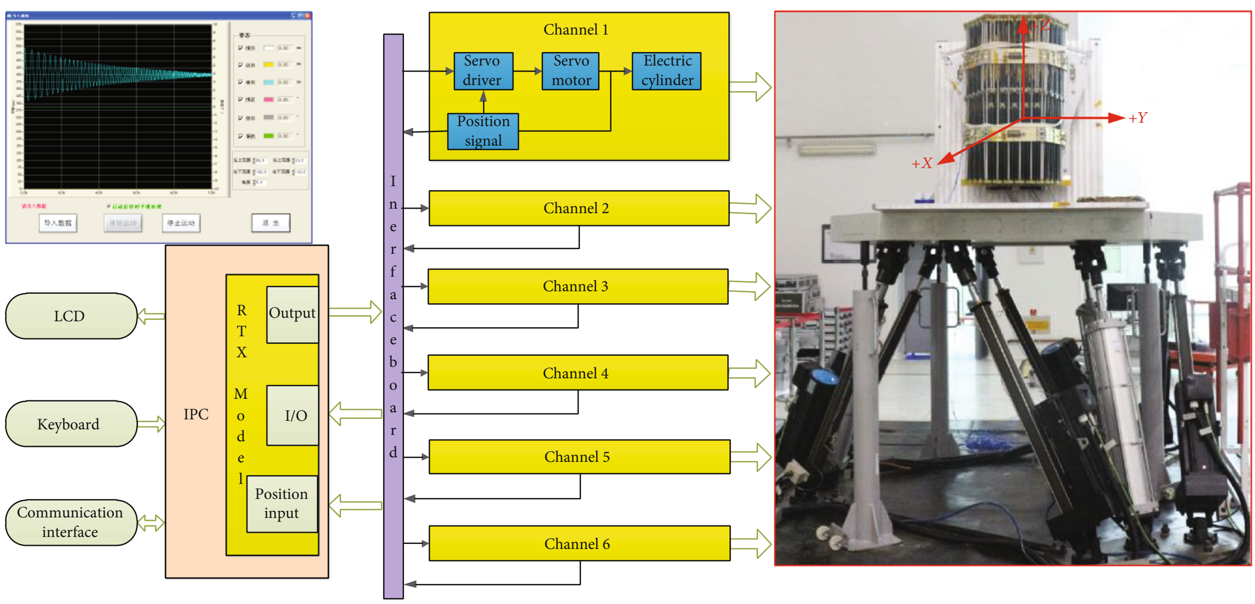

FIGURE 6: Experimental schematic diagram of Stewart platform.

lateral movement and drive the load to realize the simulated motion.

3.2. Rotation Matrix Method. The attitude description of Stewart platform generally adopts the multirigid body rotation coordinate method [15]. In this paper, the Cardan angular coordinate is adopted based on the Cartesian coordinate system, and three coordinate axes are selected in a certain order for three consecutive rotations.

The Cardan angular coordinates are shown in Figure 4. The coordinate system $o-xyz$ first rotates the angle α around the x-axis counterclockwise to $o-xy'z'$, then rotates the angle β around the y' axis to $o-x'y'Z$, and finally rotates the angle γ around the Z-axis to the position of the coordinate system $o-XYZ$. Each rotation relationship can be described by a matrix. From the coordinate system $o-x$ yz to the coordinate system $o-xy'z'$, the point P can be expressed as (y, z) in the coordinate system $o-XYZ$ and (y', z') in the coordinate system $o-xy'z'$. The relationship is expressed by the following equation.

$$y' = Y\cos\gamma - Z\sin\gamma, \tag{1}$$

$$z' = Y\sin\gamma + Z\cos\gamma. \tag{2}$$

In matrix form,

$$\begin{bmatrix} x \\ y \\ z \end{bmatrix} = \begin{bmatrix} 1 & 0 & 0 \\ 0 & \cos\alpha & -\sin\alpha \\ 0 & \sin\beta & \cos\alpha \end{bmatrix} \begin{bmatrix} x \\ y' \\ z' \end{bmatrix}. \tag{3}$$

Similarly,

$$\begin{bmatrix} x \\ y' \\ z' \end{bmatrix} = \begin{bmatrix} \cos\beta & 0 & \sin\beta \\ 0 & 1 & 0 \\ -\sin\beta & 0 & \cos\beta \end{bmatrix} \begin{bmatrix} x' \\ y' \\ Z \end{bmatrix}, \tag{4}$$

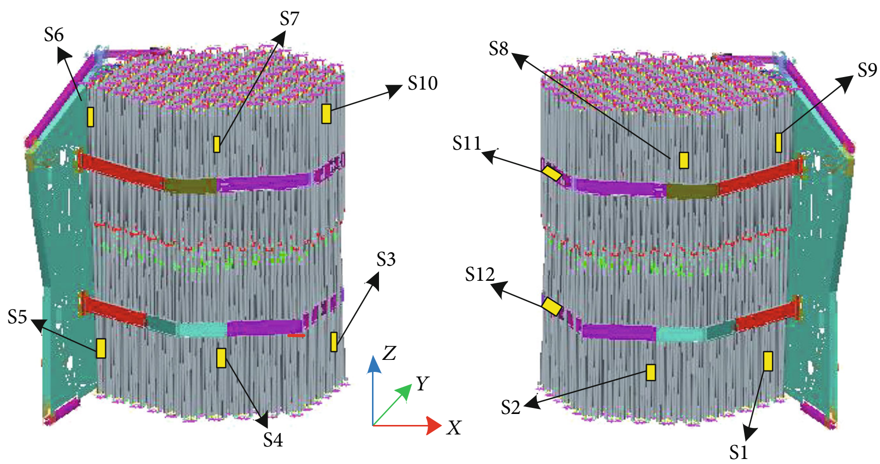

Figure 7: Measuring points on the antenna.

$$\begin{bmatrix} x' \\ y' \\ Z \end{bmatrix} = \begin{bmatrix} \cos\gamma & -\sin\gamma & 0 \\ \sin\gamma & \cos\gamma & 0 \\ 0 & 0 & 1 \end{bmatrix} \begin{bmatrix} X \\ Y \\ Z \end{bmatrix}. \tag{5}$$

Therefore,

$$\begin{bmatrix} x \\ Y \\ Z \end{bmatrix} = \begin{bmatrix} c\beta c\gamma & -c\beta s\gamma & s\beta \\ c\alpha s\gamma + s\alpha s\beta c\gamma & c\alpha c\gamma - s\alpha s\beta s\gamma & -s\alpha c\beta \\ s\alpha s\gamma - c\alpha s\beta c\gamma & s\alpha c\gamma + c\alpha d\beta d\gamma & c\alpha c\beta \end{bmatrix} \begin{bmatrix} X \\ Y \\ Z \end{bmatrix}, \tag{6}$$

where c represents cos () and s represents sin ().

Therefore, the vector between the coordinate system $o - XYZ$ and the coordinate system $o - xyz$ can be converted by the direction cosine matrix R, which can be expressed as

$$R = \begin{bmatrix} c\beta c\gamma & -c\beta s\gamma & s\beta \\ c\alpha s\gamma + s\alpha s\beta c\gamma & c\alpha c\gamma - s\alpha s\beta s\gamma & -s\alpha c\beta \\ s\alpha s\gamma - c\alpha s\beta c\gamma & s\alpha c\gamma + c\alpha d\beta d\gamma & c\alpha c\beta \end{bmatrix}. \tag{7}$$

3.3. Inverse Kinematics of Stewart Platform. To accurately control the position and attitude of Stewart platform, the six cylinders' length needs to be solved according to the predetermined position and attitude of the upper load platform, namely, three linear coordinate parameters (x, y, z) and three rotational coordinate parameters (α, β, γ).

Two reference points O_p and O_b, which are associated with the load platform and base platform, are selected to establish the Cartesian coordinate systems $\{P\}$ and $\{B\}$, respectively. The coordinate system $\{B\}$ is considered fixed, in which other coordinates can be represented expediently.

The vector from the origin point O_b of the coordinate system $\{B\}$ to the origin point O_p of the coordinate system $\{P\}$ can be represented as t, where $t = (x, y, z)$. The Cardan angle between $\{P\}$ and $\{B\}$ is θ, where $\theta = (\alpha, \beta, \gamma)$.

Table 1: Input conditions for low-frequency vibration test.

Direction	Frequency (Hz)	Magnitude
Z	0.4 ~ 1.8	0.04~0.45 g
	1.8 ~ 6	0.45 g
	6 ~ 8	0.45~0.65 g
X	0.4 ~ 2.1	0.1 ~ 0.33 g
	2.1 ~ 8 Hz	0.33 g
Y	0.8 ~ 5	0.2 g
Scanning rate	0.05 Hz/s	

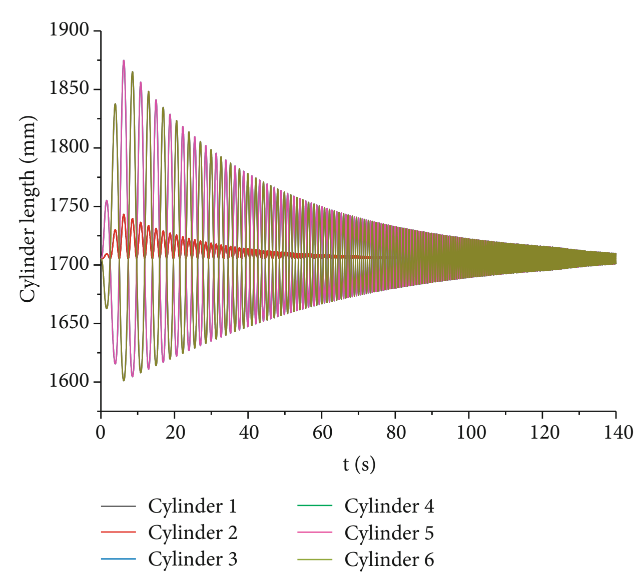

Figure 8: Motion curves of the six cylinders during the test in the X -direction.

It is assumed that the vector from O_p to the connection point between the load platform and each electric cylinder is P_i, the vector from O_b to the connection point between the base platform and each cylinder is b_i, and the vector of the connection points at both ends of the six cylinders is S_i,

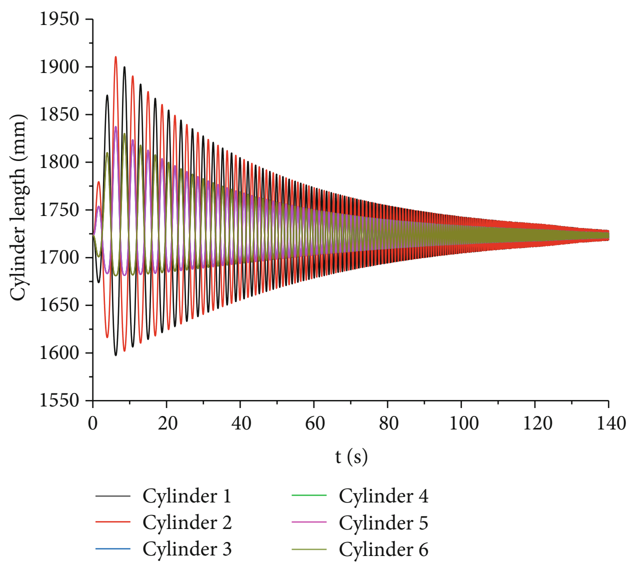

Figure 9: Motion curves of the six cylinders during the test in the Y -direction.

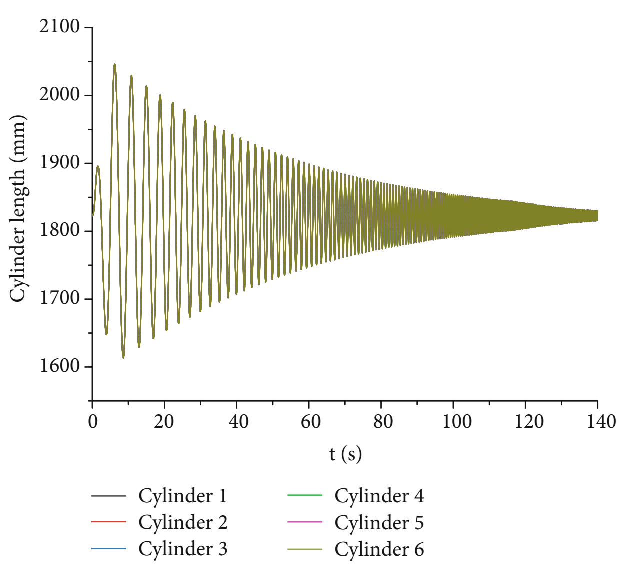

Figure 10: Motion curves of the six cylinders during the test in the Z-direction.

and the relation between the vectors above can be illustrated in Figure 5.

Then, the following formula can be obtained:

$$S_i = Rp_i + t - b_i, \tag{8}$$

where R is the rotating cosine matrix ($i = 1, 2, 3, 4, 5, 6$).

The length of electric cylinder is

$$L_i = \|S_i\| = \frac{(Rp_i + t - b_i)}{\|Rp_i + t - b_i\|} L_i = \|S_i\|. \tag{9}$$

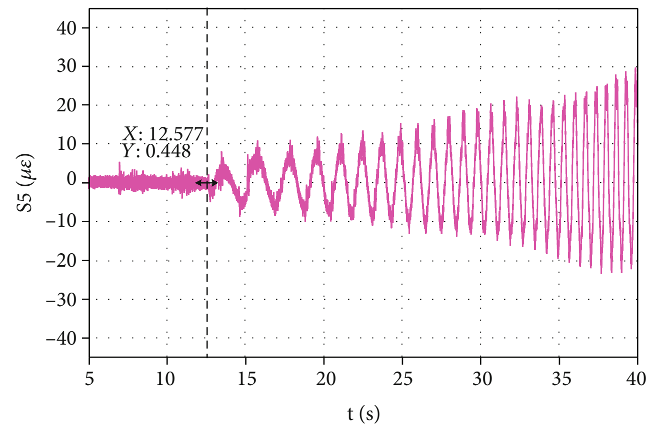

Figure 11: Response curve of point S5 in X-direction vibration.

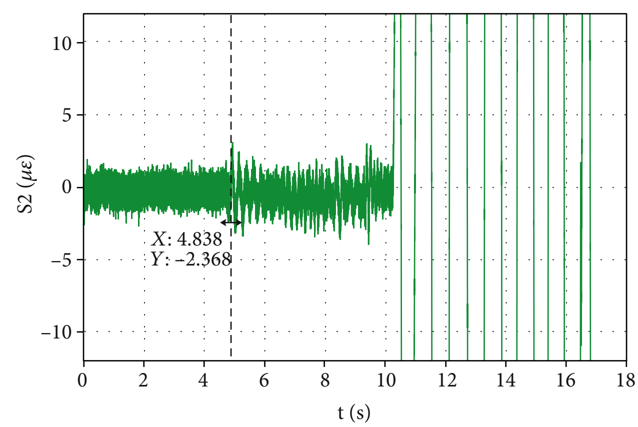

Figure 12: Response curve of point S2 in Y-direction vibration.

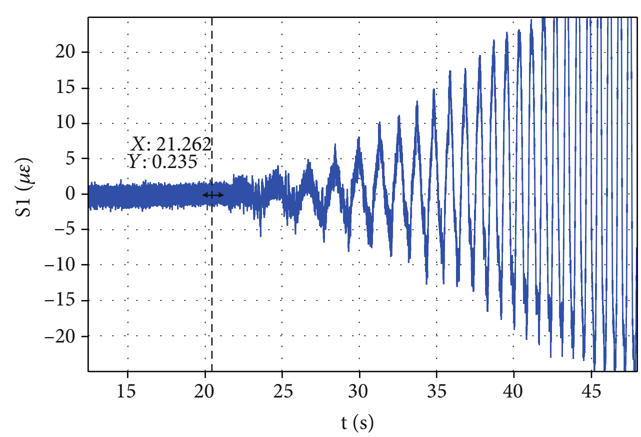

Figure 13: Response curve of point S1 in Z-direction vibration.

And the unit vector of S_i is

$$s_i = \frac{S_i}{\|S_i\|}. \tag{10}$$

The formula above establishes the relationship between the pose of the load platform and the cylinder, that is, the inverse kinematics of Stewart platform.

Table 2: Test result of each measuring point in X-direction.

Measuring point	X-direction Amplitude ($\mu\varepsilon$)		Time (s) Initial time	First peak time	Initial frequency (Hz)	Fundamental frequency (Hz)
S1	-50	42.9	12.6	91	0.4	4.02
S2	-79.8	29.7		92.7		
S3	-104.1	54.6		74.8		
S4	-89	51		82		
S5	-82.3	86		80.3		
S6	-276	40		90		
S7	-134	87		86		
S8	-75	137		100		
S9	-22	41		91.9		
S10	-157	344		85		
S11	-27	85		91.9		
S12	-29	46		92.6		
Dynamic displacement	dx: -8.2 ~ 8.75 mm; dy: -4.1 ~ 4.3 mm; dz: -61.8 ~ 64.3 mm					

Table 3: Test result of each measuring point in Y-direction.

Measuring point	Y-direction Amplitude ($\mu\varepsilon$)		Time (s) Initial time	First peak time	Initial frequency (Hz)	Fundamental frequency (Hz)
S1	-68.4	119	9.8	22.2	0.8	1.51
S2	-46	20		22.9		
S3	-120	16		22.2		
S4	-110	22		22.9		
S5	-64	123		20.1		
S6	-179	102		21.3		
S7	-439	38		24.0		
S8	-374	195		24.0		
S9	-9.6	148		23.3		
S10	-12	268		22.9		
S11	-9.6	40		22.2		
S12	-33.5	59		22.2		
Dynamic displacement	dx: -1.73~12.37 mm; dy: -140.6 ~ 117.1 mm; dz: -6.76~3.67 mm					

The Jacobian matrix is related to the cylinder extension velocity S_i and the velocity vector $\dot{\chi}$, and the attitude of the load platform is a function of $(x, y, z, \alpha, \beta, \gamma)$, then,

$$\begin{aligned} \omega &= \dot{\theta}, \\ \nu &= \dot{t}, \\ \dot{\chi} &= \left(\nu^T \omega^T\right)^T, \\ q_i &= R p_i. \end{aligned} \tag{11}$$

The sliding speed of each cylinder is

$$\dot{S}_i = s_i(\nu + \omega \times q_i) = \left(s_i^T (q_i \times s_i)^T\right) \begin{pmatrix} \nu \\ \omega \end{pmatrix} = J\dot{\chi}. \tag{12}$$

Then, the Jacobian matrix is

$$J = \left(s_i^T (q_i \times s_i)^T\right). \tag{13}$$

4. Low-Frequency Vibration Test

A low-frequency vibration test system based on 6-DOF Stewart platform is established as shown in Figure 6. In the system, the main function of the electrical control part is to receive the command data output by the control system and transmit it to the servo driver. The signal is amplified to control the motor movement, which will drive the electric cylinder to realize various postures of the platform.

In the test, the truss antenna is installed on the platform, and the vibration load acts on the platform along three mutually orthogonal directions, respectively. The measuring points on the structure are showed in Figure 7.

Table 4: Test result of each measuring point in Z-direction.

Measuring point	Z-direction Amplitude ($\mu\varepsilon$)		Time (s) Initial time	First peak time	Initial frequency (Hz)	Fundamental frequency (Hz)
S1	-29.7	33.5		87.4		
S2	-45.7	42.6		110.6		
S3	-45.4	83.2		94.4		
S4	-129.4	161.7		88.4		
S5	-48.4	78.7		95.3		
S6	-365.1	255.7	21.31	93.7	0.4	4.02
S7	-167	276.9		94.0		
S8	-298.2	98.8		93.6		
S9	-39.3	33.8		93.9		
S10	-109.7	215.9		93.8		
S11	-21.8	23.4		94.0		
S12	-47.2	17.3		93.9		
Dynamic displacement	dx: -8.7 ~ 9.25 mm; dy: -4.6 ~ 4.6 mm; dz: -62.4 ~ 65.1 mm					

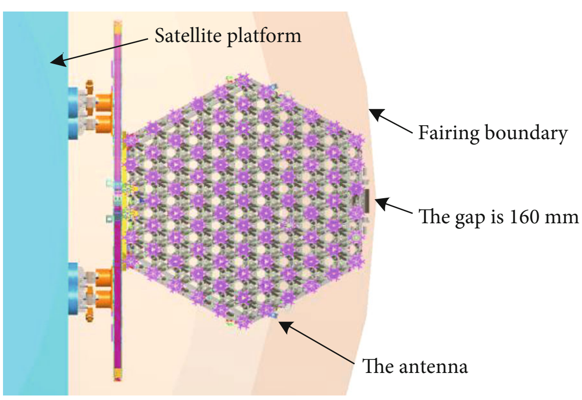

Figure 14: Installation status of antenna in the fairing.

The test conditions are determined as shown in Table 1. Moreover, a constant frequency vibration test was carried out at 1.5 Hz with 0.2 g load according to the actual needs.

Figures 8–10 show the motion curves of the six cylinders during the vibration test.

The following figures (Figures 11–13) show the response curve in each direction during the vibration, and the tables (Tables 2–4) give the maximum strain and dynamic displacement response and fundamental frequency information of the above main measuring points. The fundamental frequency information is obtained by time conversion, and the dynamic displacement is obtained by high-speed photogrammetry system, and the measurement accuracy is better than 0.1 mm.

According to the test results, the response in X-direction and Z-direction of the truss antenna is coupled, and the fundamental frequency is 4.02 Hz, while the fundamental frequency in Y-direction is the lowest, which is 1.51 Hz as shown in Figure 3 and Table 4. The maximum dynamic displacement of the antenna is 140.6 mm. Figure 14 shows the gap between the antenna and the fairing in a certain application, which is much greater than the dynamic displacement.

5. Conclusion

The truss deployable antenna has the remarkable characteristics of low fundamental frequency and flexible nonlinearity, which makes it difficult to use the conventional shaking table to investigate the vibration characteristics in the low frequency band. In this paper, a low-frequency test system based on 6-DOF Stewart parallel platform is established, and the structural characteristics of the antenna in the stowed state below 2 Hz are analyzed. It shows that the lowest fundamental frequency is 1.51 Hz in Y-direction and the dynamic displacement is 140.6 mm. The results are of great value to the further engineering application of the antenna.

Data Availability

The data that support the findings of this study are available from China Academy of Space Technology (Xi'an). Restrictions apply to the availability of these data, which were used under license for this study. Data are available from the authors with the permission of our constitution.

Conflicts of Interest

The authors declare that they have no conflicts of interest.

Acknowledgments

This work was supported by the National Natural Science Foundation of China (NNSFC) under Grant No. 11290154 and No. U1537213.

References

[1] X. Y. Chen and F. L. Guan, "A large deployable hexapod paraboloid antenna," *Journal of Astronautics*, vol. 22, no. 1, pp. 75–78, 2001.

[2] Z. R. Huang, Y. P. Song, and S. K. Zheng, "Analysis of configuration design and deployable coordination of offset—fed

truss reflector," *Mechanical Science and Technology for Aerospace Engineering*, vol. 11, pp. 1791–1796, 2016.

[3] R. Q. Liu, D. K. Tian, Z. Q. Deng, H. W. Guo, and Z. J. Liu, "Kinematics modeling and driving spring design of truss structure for deployable truss antenna," *Advanced Materials Research*, vol. 457, pp. 1337–1341, 2012.

[4] Z. H. Qi, J. H. Chang, and G. Wang, "Analysis and control of deployment process for hoop truss deployable antenna," *Journal of Astronautics*, vol. 35, no. 1, pp. 61–68, 2014.

[5] M. Akira, I. Hironori, and T. Akio, "Study on ground verification for large deployable modular structures," *Journal of Spacecraft & Rockets*, vol. 43, no. 4, pp. 780–787, 2006.

[6] J. W. Guo, Y. S. Zhao, X. D. Xun, and Y. J. Li, "Design and analysis of truss deployable antenna mechanism based on a novel symmetric hexagonal profile division method," *Chinese Journal of Aeronautics.*, vol. 34, no. 8, pp. 87–100, 2021.

[7] M. L. Zhao and F. L. Guan, "Kinematic analysis deployable toroidal spatial truss structures for large mesh antenna," *Journal Of The International Association For Shell And Spatial Structures*, vol. 46, no. 3, pp. 195–204, 2005.

[8] J. A. Fager, "Large space erectable antenna stiffness requirements," *Journal of Spacecraft & Rockets*, vol. 17, no. 2, pp. 86–93, 2015.

[9] Z. R. Huang, S. K. Zheng, J. L. Zhu, and C. Guo-Ding, "Design optimization of expansion driven components for the HJ-1-C satellite," *Journal of Radars*, vol. 3, no. 3, pp. 282–287, 2014.

[10] X. S. Jin, "The environmental testing of spacecrafes and its developing trends," *Spacecraft Environment Engineering*, vol. 19, pp. 12–18, 2002.

[11] F. Hu, Y. P. Song, S. K. Zheng, Z. Huang, and J. Zhu, "Advances and trends in space truss deployable antenna," *Journal of Astronautics*, vol. 39, no. 2, pp. 111–120, 2018.

[12] L. Liu, *Design and Development on Linear Vibratior with Low-Frequency of Aerospace Products Testing [M.S. thesis]*, Harbin Institute of Technology, Harbin, China, 2015.

[13] A. Preumont, M. Horodinca, I. Romanescu et al., "A six-axis single-stage active vibration isolator based on Stewart platform," *Journal of Sound and Vibration*, vol. 300, no. 3-5, pp. 644–661, 2007.

[14] D. Kamesh, R. Pandiyan, and A. Ghosal, "Modeling, design and analysis of low frequency platform for attenuating micro-vibration in spacecraft," *Journal of Sound and Vibration*, vol. 329, no. 17, pp. 3431–3450, 2010.

[15] C. Qian, E. Jia-qiang, L. Ming, D. Yuan-wang, and Z. Mao, "Vibration analysis of the dynamic model of Stewart platform with six degrees of freedom," *Journal of Hunan University (Natural Sciences)*, vol. 43, no. 2, pp. p36–p42, 2016.